

ASVD: Activation-aware Singular Value Decomposition for Compressing Large Language Models

Zhihang Yuan*
Houmo AI
hahnyuan@gmail.com

Yuzhang Shang*
Illinois Institute of Technology
yshang4@hawk.iit.edu

Yue Song
University of Trento
yue.song@unitn.it

Qiang Wu
Houmo AI
qiang.wu@houmo.ai

Yan Yan
Illinois Institute of Technology
yyan34@iit.edu

Guangyu Sun
Peking University
gsun@pku.edu.cn

Abstract

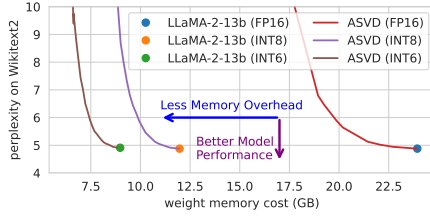
In this paper, we introduce a new post-training compression paradigm for Large Language Models (LLMs) to facilitate their wider adoption. We delve into LLM weight low-rank factorization, and find that the challenges of this task stem from the outlier phenomenon in the LLM activations and the sensitivity difference among various kinds of layers. To address these issues, we propose a training-free approach called Activation-aware Singular Value Decomposition (ASVD). Specifically, ASVD manages activation outliers by scaling the weight matrix based on the activation distribution, thereby enhancing decomposition accuracy. Additionally, we propose an efficient iterative calibration process to optimize layer-specific decomposition by addressing the varying sensitivity of different LLM layers. ASVD can compress a network by 10-20%, without compromising the performance of LLMs. Based on the success of the low-rank decomposition of projection matrices in the self-attention module, we further introduce ASVD to compress the KV cache. By reducing the channel dimension of KV activations, memory requirements for KV cache can be largely reduced. Thanks to the 50-75% reduction in the rank of the KV projection matrices, ASVD can further achieve 50% KV cache reductions without performance drop in a training-free manner. Code and compressed models are available at [ASVD4LLM](#).

1 Introduction

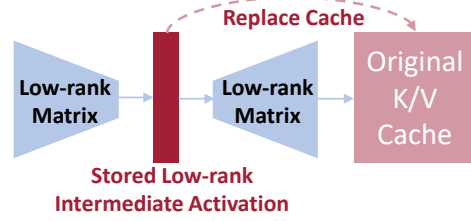
Numerous strategies have been proposed to address the memory consumption challenges in Large Language Models (LLMs), as reviewed by [Ding et al. \[2023\]](#), [Zhu et al. \[2023\]](#). In the realm of LLM compression, various techniques have been extensively explored, including weight quantization [[Dettmers et al., 2022](#)], network pruning [[Frantar & Alistarh, 2023](#)], and knowledge distillation [[Agarwal et al., 2023](#)]. Distinct from these approaches, the paradigm of low-rank matrix decomposition is less explored but holds significant promise. Decomposition involves approximating the weight matrices in LLMs with matrices of lower rank, effectively reducing the model size. Given the massive number of parameters in LLMs, low-rank decomposition offers significant potential for memory reduction. Furthermore, low-rank decomposition can complement existing LLM compression techniques by further compressing quantized or pruned models, enhancing overall efficiency [[Cheng et al., 2017](#)]. Despite its potential, it remains a relatively underutilized approach for LLM compression.

From the perspective of network compression, traditional low-rank decomposition methods typically adhere to a straightforward process: initially training the original model and subsequently fine-tuning

*Equal Contribution.



(a) Summarized Performance of ASVD.



(b) High-level idea of using *ASVD* to compress *KV* cache.

Figure 1: (a) Our post-training LLM decomposition method is **orthogonal** to existing LLM compression techniques, enabling it to function as a versatile and plug-and-play solution for prevalent compression paradigms, including popular quantization methods. (b) By applying low-rank decomposition via *ASVD* to the Key/Value projection matrices, the original high-dimensional **KV** cache can be replaced with a low-dimensional storage.

the decomposed model [Hsu et al., 2022, Jaderberg et al., 2014, Khodak et al., 2021, Wang et al., 2021]. While this approach is effective, it is resource-intensive and requires the entire training dataset and substantial computational power for end-to-end backpropagation. Applying this method to LLMs would encounter major challenges. Firstly, the training data for LLMs may not always be readily available, often restricted by privacy and commercial considerations. Secondly, the training process for these models is notoriously expensive, both in terms of time and computational resources. Given these constraints, the concept of “training-free” compression emerges as a more viable approach for LLMs [Zhu et al., 2023]. This approach includes methods like LLM post-training quantization [Dettmers et al., 2022, Yuan et al., 2023] and LLM post-training pruning [Frantar & Alistarh, 2023], which compress LLMs without the need for extensive retraining. These training-free (*i.e.*, *post-training*) methods offer a more practical solution for efficiently compressing LLMs.

To realize **LLM low-rank decomposition in a training-free manner**, we conduct an extensive analysis of the baseline methods for LLM decomposition. We first observe that straightforward application of existing low-rank decomposition techniques, which typically necessitate training, turns out ineffective for LLMs [Denton et al., 2014, Jaderberg et al., 2014, Khodak et al., 2021, Lebedev et al., 2014, Moczulski et al., 2015, Sainath et al., 2013, Wang et al., 2021]. Digging into the failures, we reveal several challenges unique to post-training decomposition for LLMs. One key challenge involves managing outliers in the activations, which significantly intensifies the decomposition error. This challenge echoes findings in LLM quantization research [Kim et al., 2023, Lin et al., 2023], highlighting the importance of handling such outliers in LLMs.

To address these challenges, we propose Activation-aware Singular Value Decomposition (ASVD), where the distribution of activations are considered into the weight decomposition process. Specifically, it achieves this by scaling the values in the weight matrix column-wisely, based on the distribution patterns observed across input and output channels. This adjustment proves particularly beneficial for channels with outlier activations, allowing the ASVD to allocate enhanced focus to these specific weights. Such targeted adjustment facilitates a more accurate reconstruction of the weight matrix, thereby minimizing prediction errors and improving the overall efficiency of the decomposition process. We further investigate the varying sensitivity of different LLM layers to decomposition. We find that weights in Multi-Head Attention layers [Vaswani et al., 2017] tend to be more resilient to decomposition compared to those in Multi-Layer Perceptron layers. This sensitivity variability across layers prompts us to develop a method to assign the compression ratio for each layer. ASVD assesses each layer’s sensitivity to decomposition at different ranks, enabling us to assign a suitable rank for optimal decomposition. Note that this probing assess is very efficient, requiring only a limited sample set for evaluation.

Empirically, we evaluate ASVD with LLaMA and LLaMA-2 [Touvron et al., 2023a,b]. Our experiments reveal that ASVD can reduce the rank of the weight matrix by 50-75% (corresponds to 10-20% compression ratio), with only a marginal 1% accuracy loss on benchmarks like MMLU [Hendrycks et al., 2020]. We also validate ASVD is compatible with 4/6/8-bit quantization, as shown in Fig. 1a.

Importantly, leveraging the successful low-rank decomposition of projection matrices in the self-attention module, we can integrate ASVD with KV cache compression. Specifically, by applying ASVD to decompose the Key/Value projection matrices, we can derive low-rank intermediate activations that serve as replacements for the KV cache stored in high-dimension space as shown in Fig. 1b. This substitution significantly reduces the memory usage of the KV cache, enabling support for larger

batch sizes or longer sequence lengths, which are essential for real-world applications [Yuan et al., 2024]. In practice, by replacing the KV cache with low-rank intermediate activations, we can reduce up to 50% of the memory consumption of KV cache.

2 Related Work

Large Language Model Compression. The field of model compression for Large Language Models (LLMs) has seen a surge of innovative techniques aimed at mitigating the substantial computation and memory requirements these models demand [Yuan et al., 2024, Zhu et al., 2023]. Various methods have emerged to address this challenge, each taking a unique approach to reduce the memory footprint of LLMs. These methods primarily fall into three categories: weight quantization [Courbariaux et al., 2015, Dettmers et al., 2022], network pruning [Frantar & Alistarh, 2023, LeCun et al., 1989], and knowledge distillation [Agarwal et al., 2023, Hinton et al., 2015]. For the wide body of research on LLM compression, please refer to [Zhu et al., 2023] for the comprehensive survey. Among these methods, weight quantization has gained significant traction in the context of LLMs due to its effectiveness. However, despite its popularity as a neural network compression technique, low-rank factorization has not been extensively explored in the realm of LLMs.

Low-rank Decomposition. In the realm of low-rank decomposition [Schotthöfer et al., 2022] for neural network compression, existing methods can be broadly classified into two categories: **fixed low rank** and **variable low rank** approaches. Fixed rank methods typically involve decomposing weight matrices of pre-trained networks using techniques like Singular Value Decomposition (SVD) or tensor decomposition, followed by fine-tuning the factorized network [Denton et al., 2014, Lebedev et al., 2014, Moczulski et al., 2015, Sainath et al., 2013]. They also involve constraining weight matrices to maintain a fixed low rank during training [Jaderberg et al., 2014, Khodak et al., 2021, Wang et al., 2021], or constructing layers as linear combinations of layers with varying ranks [Ioannou et al., 2015]. A notable limitation of these methods is the introduction of matrix decomposition rank as an additional hyperparameter requiring fine-tuning. In contrast, rank-adaptive methods address this limitation by automatically determining and adjusting the low-rank structure. In particular, Kim et al. [2019, 2015] apply heuristics search to pre-determine the decomposition rank, while Wen et al. [2017] learn low-rank weights through a loss function penalizing approximated matrix ranks. Li et al. [2023] use low-rank approximation plus a sparse matrix to compress the weight matrix in transformers.

However, none of these methods have worked in the era of LLMs due to their training-require nature. In this work, we introduce ASVD, a *post-training* LLM decomposition approach enabling the adaptive determination of SVD ranks to optimize the matrix approximations based on feature activations. To our knowledge, this is the first attempt to compress the weights of LLMs through decomposition in a training-free manner.

3 Method

3.1 Naïve SVD for Compressing Weight Matrix

Singular Value Decomposition (SVD) can be used to decomposing the weights of linear layers, which involves decomposing a weight matrix $\mathbf{W} \in \mathbb{R}^{m \times n}$ into three matrices: \mathbf{U} , $\mathbf{\Sigma}$, and \mathbf{V}^T , such that $\mathbf{W} \approx \mathbf{W}\mathbf{\Sigma}\mathbf{V}^T$, where $\mathbf{\Sigma}$ is an $m \times n$ diagonal matrix, the diagonal values in $\mathbf{\Sigma}$ are the singular values of \mathbf{W} , and $\mathbf{U} \in \mathbb{R}^{m \times m}$ and $\mathbf{V} \in \mathbb{R}^{n \times n}$ are corresponding right and left singular vector matrices, respectively [Demmel, 1997].

The SVD compression process for a weight matrix can be summarized in three steps: **Decomposition:** Factorize \mathbf{W} using SVD. **Truncation:** Retain the top k singular values and their corresponding right and left singular vectors. This results in approximated matrices \mathbf{U}_k , $\mathbf{\Sigma}_k$, and \mathbf{V}_k^T , where the right singular vector matrix \mathbf{U}_k is $m \times k$, singular $\mathbf{\Sigma}_k$ is $k \times k$, and left singular vector matrix \mathbf{V}_k^T is $k \times n$. The choice of k is critical in balancing the compression ratio and the compressed model’s performance. **Reconstruction:** Reconstruct an approximated weight matrix: $\mathbf{W}_k = \mathbf{U}_k\mathbf{\Sigma}_k\mathbf{U}_k^T$.

3.2 Challenges of Compressing LLMs via SVD

Decomposing the large matrices in LLMs (e.g., 4096×4096 matrices ubiquitous in LLaMA-7b [Touvron et al., 2023a]) into lower ranks presents a viable pathway for model compression. However, straightforward application of existing low-rank decomposition techniques [Denton et al.,

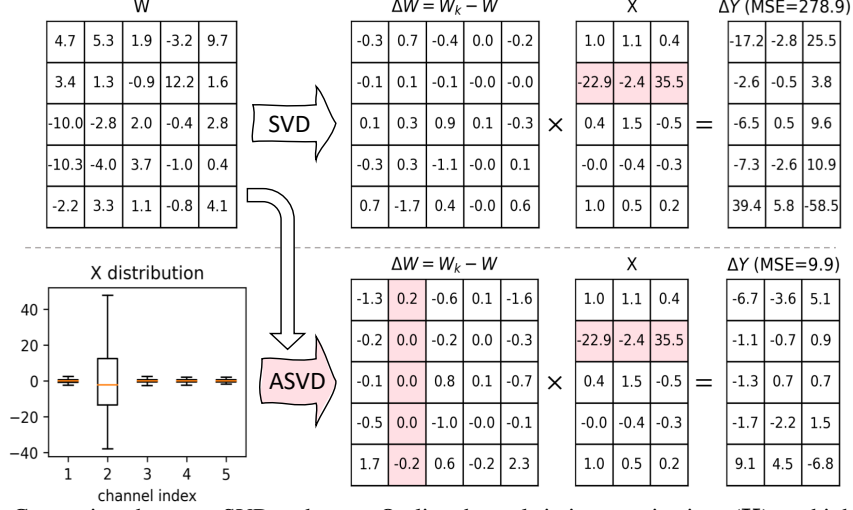


Figure 2: Comparison between SVD and ASVD. Outlier channels in input activations (X) are highlight in red, and ASVD takes these into consideration, which can contribute to a reduction in output error.

2014, Khodak et al., 2021, Lebedev et al., 2014, Li et al., 2023, Moczulski et al., 2015, Wang et al., 2021], which typically necessitate training, proves ineffective for LLMs.

Challenge 1: Influence of Activation: This perspective shifts the focus from solely relying on the truncation error L_t , which depends only on the model’s weights, to also accounting for the activations. The rationale behind this is the critical role of outliers in activations within LLMs [Kim et al., 2023, Lin et al., 2023, Wei et al., 2022]. Thus, for effective LLM decomposition, our objective optimization becomes:

$$\begin{aligned} \mathbf{W}_k^* &= \arg \min_{\mathbf{W}_k} \mathcal{L}(\mathbf{W}_k), \\ \arg \min_{\mathbf{W}_k} \mathcal{L}(\mathbf{W}_k) &= \|\mathbf{W}_k \mathbf{X} - \mathbf{W} \mathbf{X}\| \end{aligned} \quad (1)$$

Here, \mathbf{X} represents the input activations, which are cached from a small calibration set. This set is derived from the pre-training dataset to avoid overfitting to a specific task. Essentially, our objective is to ensure that the output of the decomposed LLM closely mimics the output of the original LLM, rather than merely aligning their weights. This approach prioritizes functional equivalence over structural similarity, recognizing that accurate output replication is more critical for maintaining the model’s post-decomposition performance. We define the variation in activations between the compressed matrix \mathbf{W}_k and the original matrix \mathbf{W} as:

$$\Delta \mathbf{Y} = (\mathbf{W}_k - \mathbf{W}) \mathbf{X}. \quad (2)$$

To illustrate this concept, we visualize an example of \mathbf{W} , \mathbf{W}_k (decomposed by simply SVD), \mathbf{X} , and the resulting variation in activations $\Delta \mathbf{Y}$ in Fig. 2 (Top line). This visualization reveals a critical insight: even when the variation in weights $\Delta \mathbf{W} = \mathbf{W} - \mathbf{W}_k$ is relatively minor, the corresponding variation in activations $\Delta \mathbf{Y}$ can be huge. This significant variation in activations is a key factor in why a straightforward SVD-based decomposition approach falls short in effectively decomposing LLMs. The activation variations, despite being derived from input activations of large magnitude (not the weight variations), can lead to considerable changes in the whole model’s output, thereby undermining the decomposition’s efficacy.

Challenge 2: Singular Values Variations among Layers: The distribution of singular values within a matrix is indicative of its sparsity and, by extension, its sensitivity to certain types of information [Kim et al., 2019, 2015, Wen et al., 2017]. In LLMs, there is a notable variation in singular values across different layers. Specifically, some layers exhibit a concentration of large singular values, signifying less sensitivity to weight variation. This characteristic often correlates with these layers being easy to compress. Conversely, other layers in the LLMs display a more uniform distribution of smaller singular values. Such a pattern suggests a balanced contribution from various singular vector pairs. This variability in the distribution of singular values among layers presents a unique challenge, as it implies that each layer may require a tailored approach to decompose and maintain the overall functionality of the LLM.

These challenges underscore the necessity for innovative approaches specifically designed for the LLM decomposition. Our objective is to achieve efficient compression while circumventing the substantial computational and data demands associated with training-based methods. To address the first challenge, we introduce an Activation-aware SVD mechanism, which is detailed in Section 3.3. This method is designed to mitigate the impact of weight variation on activations. For the second challenge, we propose a Sensitivity-based Truncation Rank Searching mechanism, elaborated in Section 3.5, which adapts to the varying singular value distributions among different layers.

3.3 ASVD: Activation-aware Singular Value Decomposition

Our ASVD is designed to refine the weight matrix \mathbf{W} in LLMs by taking into account the effect of input activation channels. The process comprises the following three steps:

Scaling the Weight Matrix. The first step involves scaling the weight matrix \mathbf{W} by a diagonal matrix \mathbf{S} . This matrix \mathbf{S} is constructed to represent the impact of input channels on the weights, essentially adjusting \mathbf{W} to better adapt with the activation patterns of the input \mathbf{X} , as demonstrated in Fig. 2 (Bottom line). The scaled weight matrix is denoted as \mathbf{WS} , and the equation is formulated as:

$$\mathbf{W} = \mathbf{WSS}^{-1} = (\mathbf{WS})\mathbf{S}^{-1}. \quad (3)$$

This scaling step is crucial as it modifies the weight matrix to reflect the varying significance of different input channels, making the decomposition more effective and targeted.

Applying SVD to the Scaled Matrix. After scaling the weight matrix, the next step is to apply SVD to the scaled matrix \mathbf{WS} . The SVD of \mathbf{WS} is expressed as $\mathbf{WS} = \mathbf{U}'\mathbf{\Sigma}'\mathbf{V}'^T$. To realize the matrix compression, we truncate this decomposition to retain only the first k singular values and corresponding vectors. The truncated form of the decomposition is represented as:

$$\mathbf{WS} \approx \mathbf{U}'_k \mathbf{\Sigma}'_k \mathbf{V}'_k{}^T. \quad (4)$$

This step is pivotal as it ensures that the most significant aspects of the scaled weight matrix are retained. While less critical information, which contributes minimally to the model's output, is discarded.

Reconstructing the Approximated Weight Matrix. The final step in the ASVD process is to reconstruct an approximation of the original weight matrix. This reconstruction is accomplished by multiplying the truncated decomposition $\mathbf{U}'_k \mathbf{\Sigma}'_k \mathbf{V}'_k{}^T$ with the inverse of the scaling matrix \mathbf{S}^{-1} . The multiplication of $\mathbf{V}'_k{}^T$ with \mathbf{S}^{-1} yields a new matrix $\mathbf{V}''_k{}^T$ (i.e., $\mathbf{V}''_k{}^T = \mathbf{V}'_k{}^T \mathbf{S}^{-1}$), which is the transformed version of the truncated right singular vectors considering the scaling effect. As a result, the final approximated weight matrix can be expressed as:

$$\mathbf{W} \approx \mathbf{U}'_k \mathbf{\Sigma}'_k \mathbf{V}''_k{}^T. \quad (5)$$

ASVD focus on channel-wise activation outliers, striving to mitigate these outliers by appropriately scaling the corresponding weights. In this way, the activation variation can be mitigated as illustrated in Fig. 2. Note that the diagonal nature of \mathbf{S} simplifies its inversion process, making \mathbf{S}^{-1} computationally efficient. The subsequent challenge is to devise a method or criteria for accurately determining \mathbf{S} so that it effectively aligns with the activation patterns observed in the LLM, ensuring that the scaling process optimally addresses the outlier activations.

Setting Scaling Matrix \mathbf{S} . Each diagonal element in the scaling matrix \mathbf{S} , particularly \mathbf{S}_{ii} is pivotal in modulating the input activations as $(\mathbf{WS})\mathbf{X}$. Each entry of \mathbf{S}_{ii} specifically scales the influence of the i -th input channel. This scaling is instrumental in adjusting how each activation channel impacts the weight matrix during the decomposition process. The significance of \mathbf{S}_{ii} is visualized in Fig. 2 (bottom line), where its role in modulating channel influence is depicted. We use absolute mean value of input activation to set \mathbf{S}_{ii} . We calculate \mathbf{S}_{ii} by calculating the absolute mean value of the activations in the i -th channel. Mathematically, if $\mathbf{X}_{i,:}$ represents the input activation values of the i -th channel, then \mathbf{S}_{ii} is computed as: $\mathbf{S}_{ii} = (\frac{1}{n} \sum_{j=1}^n |\mathbf{X}_{ij}|)^\alpha$, where n is the total number of activations for the i -th channel and hyper-parameter α provides flexibility to adjust the level of activation sensitivity incorporated into the scaling. This method focuses on the average magnitude of activation in each channel, capturing the general intensity of activation signals irrespective of their positive or negative nature.

3.4 KV Cache Compression

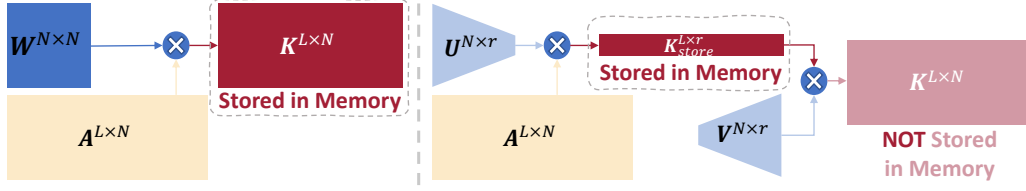


Figure 3: **A demonstration of how ASVD reduces the memory cost of the K cache.** (Left) With long text lengths L , the memory required for storing the K cache in a N -dimensional space becomes substantial. (Right) ASVD decomposes the key projection weight matrix \mathbf{W} into two low-rank matrices \mathbf{U} and \mathbf{V} (see Sec. 3.3). This low-rank structure allows the K representation to be stored in a reduced r -dimensional space, where $r \ll N$. Consequently, we only need to save the intermediate K in the r dimension instead of N dimension, saving the K cache $\frac{N}{r}$ times. Note that saving V cache is the same, and when content length L becomes really large (e.g., 1M tokens) or with larger batch size, the KV cache becomes a significant factor in memory cost.

LLM inference with large context lengths can be incredibly resource-intensive, requiring high-end GPUs and, for the largest models, costly multi-GPU setups. Analysis of generative inference with LLMs reveals that, for relatively small batch sizes, the computation is primarily memory-bound [Hooper et al., 2024, Liu et al., 2024]. Given the growing gap between computational speeds and memory speeds, this issue is expected to worsen over time, making it crucial to address the memory bottleneck. Further analysis indicates that the memory bottleneck is strongly correlated with context size. For long sequence lengths, the main contributor to memory consumption is the KV cache storing, so minimizing the KV cache can reduce both memory consumption and bandwidth requirements [Yuan et al., 2024].

As we discussed in Sec. 3.3, ASVD decomposes the key and value projection weight matrix $\mathbf{W} \in \mathbb{R}^{N \times N}$ into two low-rank matrices, $\mathbf{U} \in \mathbb{R}^{N \times r}$ and $\mathbf{V} \in \mathbb{R}^{N \times r}$, in a training-free manner, where N is the dimension of K/V embedding space. As shown in Fig. 3, replacing the high-rank matrix with two low-rank matrices via ASVD allows us to obtain intermediate activations in low-rank form. These intermediate activations can be stored as a replacement for the original KV cache. In other words, the original KV cache requires storing two $L \times N$ matrices. With ASVD, the new KV cache only needs to store two $L \times r$ matrices. In summary, ASVD can compress the KV cache $\frac{N}{r}$ times. This significant reduction in memory usage for the KV cache enables larger batch sizes or longer sequence lengths, which are critical for real-world applications.

3.5 Sensitivity-based Truncation Rank Searching

In addressing the second challenge, the variations of singular values among different layers of LLMs, we introduce the Sensitivity-based Truncation Rank Searching (STRS) method. This challenge arises from the fact that different layers in LLMs exhibit varying degrees of sensitivity to information compression, which is reflected in the distribution of their singular values. STRS evaluates the layer sensitivity and decides the best truncation of singular values. In the realm of NLP, perplexity is a key metric for assessing how effectively a language model predicts a sequence of tokens [Brown et al., 2020]. Therefore, we use the reduction in perplexity on the calibration dataset to evaluate the sensitivity of each layer. Similar to post-training compression methods [Dettmers et al., 2022, Frantar & Alistarh, 2023, Frantar et al., 2022], we collect a small number of input token sequences as calibration dataset.

The core of the sensitivity evaluation process involves an in-depth exploration of how the neural network reacts to varying levels of truncation. We define a set of potential truncation ratios, denoted as $R = \{0.1, 0.2, \dots, 0.9\}$. These ratios $r = \frac{km+kn}{mn}$ determine the fraction of the rank k preserved during the SVD truncation for a weight matrix with dimensions $m \times n$. For each linear layer in the LLM, we iterate through these candidate ratios. At each ratio, truncated SVD is applied to the layer’s weight matrix, temporarily replacing the original layer in the model with this decomposed version. The model’s perplexity is then evaluated on the calibration dataset.

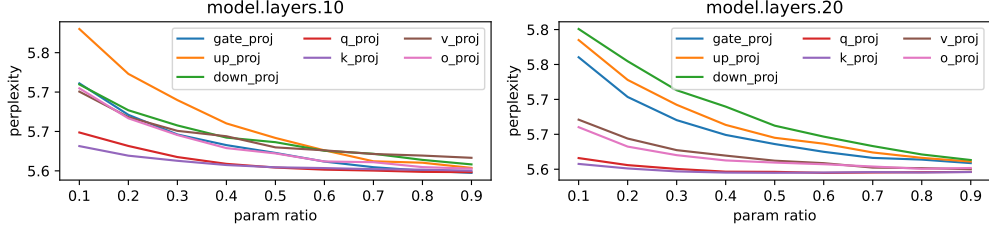


Figure 4: Perplexity across Various Linear Layers and Parameter Ratios on LLaMA-2-7b.

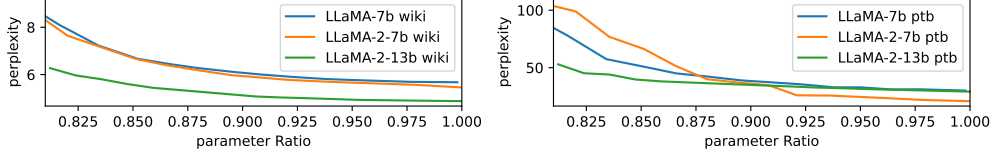


Figure 5: Perplexity trends following ASVD compression on LLaMA-2-13b, LLaMA-2-7b and LLaMA-7b.

This detailed exploration of sensitivity across various truncation levels provides essential insights into each layer’s performance dynamics, informing the optimization and decision-making processes in model compression. As illustrated in Fig. 4, there are noticeable variations in sensitivity among the different layers. Three key observations emerge from this analysis: 1. Inversely Proportional Relationship: lower parameter ratios tend to result in higher perplexity scores. 2. Higher Sensitivity in MLP Layers: MLP layers demonstrate higher sensitivity, indicating where more cautious truncation is necessary. 3. Variable Sensitivity Among Layers: Some layers exhibit relatively lower sensitivity, indicating potential for more aggressive compression.

Assuming the affects of layers are independent, we should set the truncation rank of each layer to minimize the total affect to perplexity under the constraint of parameter size. We propose a binary search algorithm to search for the best truncation rank. Detailed explanations of algorithm can be found in the Appendix.

4 Experiments

In this section, we assess the effectiveness of ASVD by conducting experiments on LLaMA [Touvron et al., 2023a] and LLaMA-2 [Touvron et al., 2023b], and presenting results on various tasks, such as Perplexity in WIKI [Merity et al., 2016] and MMLU [Hendrycks et al., 2020].

4.1 Hyper-parameters Exploration

In our study, we initiate an exploration of hyper-parameters in ASVD, focusing on the activation channel significance metric and the control factor α . This exploration is conducted on OPT-125m, a relatively small network that facilitates rapid evaluation. We rigorously explored the control factor α , and two methods for quantifying activation significance: Absolute Mean Value of Input Activation and Absolute Maximum Value of Input Activation. More details can be found in the Appendix. In summary, based on our explorations, we chose $\alpha = 0.5$ and the Absolute Mean Value method for setting the scaling matrix S in the ASVD process in the following experiments.

4.2 Parameters Compression

We conducted a comprehensive evaluation of Adaptive Singular Value Decomposition (ASVD) on two LLaMA models: LLaMA-7b and LLaMA-2-7b [Touvron et al., 2023a,b], each comprising 7 billion parameters. For each model, we selected a calibration set with 32 samples, and each sample contains 2048 tokens, from the Wikitext dataset to assess the layer-wise sensitivity.

ASVD involves setting varying thresholds binary searching process, enabling us to observe the impact of different compression levels on model performance. This approach resulted in a range of com-

Table 1: Performance under various compression scenarios. Param ratio indicates the proportion of parameters remaining after decomposition. MMLU results are 0-shot. SVD* means SVD using Sensitivity-based Truncation Rank Searching.

method	param ratio	LLaMA-7b			LLaMA-2-7b			LLaMA-2-13b		
		MMLU	wiki	ptb	MMLU	wiki	ptb	MMLU	wiki	ptb
original	1	30.76%	5.68	29.63	34.86%	5.47	20.82	40.16%	4.88	29.21
SVD	0.95	22.98%	2800	5458	-	nan	nan	-	nan	nan
SVD*	0.95	23.92%	136.05	183.92	24.78%	46.79	363.37	24.86%	167.63	567.02
SVD*	0.9	23.54%	698.66	262.03	24.31%	114.45	27660	-	nan	nan
ASVD	0.95	30.26%	5.78	32.64	33.24%	5.64	23.98	39.52%	4.94	31.93
ASVD	0.9	29.67%	6.09	37.80	32.58%	5.93	32.63	40.04%	5.12	34.03
ASVD	0.85	29.70%	6.80	52.11	31.57%	6.74	59.84	37.95%	5.54	39.32
ASVD	0.8	27.85%	8.89	88.09	28.15%	8.91	114.70	34.63%	6.53	59.68
ASVD	0.75	24.94%	14.51	212.80	25.97%	18.97	432.57	28.59%	8.71	110.10

Table 2: Performance under different KV cache compression ratio.

model	dataset	KV cache ratio								
		1(original)	0.9	0.8	0.7	0.6	0.5	0.4	0.3	0.2
LLaMA-2-7b	wiki	5.47	5.46	5.46	5.46	5.46	5.46	5.54	5.91	7.94
	ptb	20.82	20.86	20.86	20.86	20.86	20.86	22.21	24.90	35.08
LLaMA-2-13b	wiki	4.88	4.88	4.88	4.88	4.88	4.88	4.93	5.11	5.93
	ptb	29.21	29.10	29.10	29.10	29.10	29.10	30.55	34.18	44.65

pressed networks, each characterized by a unique compression ratio. We evaluated the performance of these compressed networks using perplexity as the primary metric, focusing on two datasets: Wikitext-2 and the Penn Treebank (PTB). The objective was to understand the relationship between compression ratio and model performance. The results, illustrated in Fig. 5, reveal several key insights: (1) As the parameter ratio decreases, there is a corresponding increase in perplexity. As more parameters are compressed, the more error is introduced by SVD. This reduces representational capacity of the network, thereby resulting in higher perplexity scores. (2) A plateau region is observed when the parameter ratio exceeds 0.9. In this range, ASVD predominantly decompresses the less sensitive layers, resulting in minimal impact on prediction accuracy. (3) Below a parameter ratio of 0.85, there is a rapid increase in perplexity, indicating that the more sensitive layers are being decompressed to a lower truncation rank, adversely affecting the model’s performance.

We also present a detailed analysis of the performance of compressed networks at various parameter ratios. This analysis aims to elucidate the impact of different compression techniques on network efficiency and accuracy. Table 1 displays the performance metrics for two LLaMA models, LLaMA-7b and LLaMA-2-7b, under several compression scenarios. These metrics include Massive Multitask Language Understanding (MMLU) zero-shot evaluation, perplexity on the Wikitext dataset (wiki), and perplexity on the Penn Treebank dataset (ptb). Our observations indicate significant variations in performance as a function of the parameter ratio and the compression method employed. Specifically, the table highlights the performance of each model when using standard SVD, SVD with binary search for truncation ranks (SVD*), and ASVD at different parameter ratios ranging from 0.75 to 0.95.

4.3 KV Cache Compression

We evaluate the KV Cache compression by using ASVD to decompose k projection and v projection in transformer. Table 2 summarizes the results, showing the perplexities on the wikitext2 and Penn Treebank datasets for different KV cache compression ratios. It is evident that the perplexity values remain stable when the KV cache ratio is above 40%. When the ratio is lower than 40%, the performance of the network is decreased. These observations suggest that ASVD is effective to compress the KV cache without negatively impacting the model.

Table 3: Combining weight quantization with ASVD. Param ratio indicates the proportion of parameters remaining after ASVD, with 1 implying no decomposition.

param ratio	dataset	LLaMA-2-7b				LLaMA-2-13b			
		FP16	INT8	INT6	NF4	FP16	INT8	INT6	NF4
1	wiki	5.47	5.48	5.52	5.65	4.88	4.88	4.90	4.98
	ptb	20.82	20.82	20.97	22.70	29.15	29.12	29.03	30.31
0.95	wiki	5.64	5.64	5.70	5.83	4.94	4.95	4.97	5.08
	ptb	23.98	23.95	25.10	35.91	31.93	31.67	31.97	33.89
0.9	wiki	5.93	5.94	6.02	6.20	5.12	5.11	5.16	5.31
	ptb	32.63	32.19	32.83	40.82	34.03	33.64	33.66	34.93
0.85	wiki	6.74	6.73	6.90	7.43	5.54	5.56	5.62	5.90
	ptb	59.84	63.76	66.88	427.59	39.32	40.02	38.15	44.49

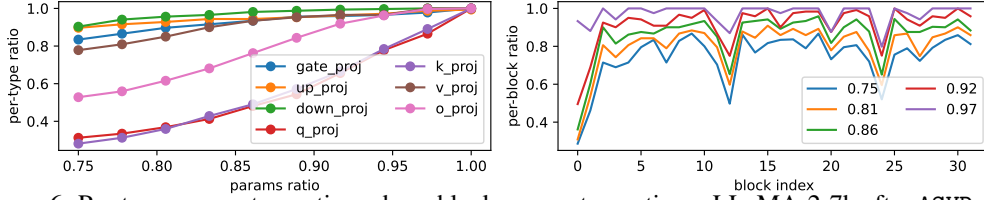


Figure 6: Per-type parameters ratio and per-block parameters ratio on LLaMA-2-7b after ASVD compression.

4.4 Integrating ASVD with Quantization

This section explores the integration of ASVD with quantization techniques to compress large language models. We investigate the synergy between ASVD and simple quantization methods, Round-To-Nearest (RTN) and 4-bit NormalFloat (NF4) [Dettmers et al., 2023], as a preliminary step. Future work could extend this investigation to more advanced quantization methods. Our experimental framework involves two stages. Firstly, we apply ASVD to decompose the network. Subsequently, we quantize the decomposed weights. We employ per-channel asymmetric quantization, targeting two quantization levels: 8-bit and 6-bit. We employ NF4 for quantizing to 4-bit.

Table 3 summarizes the results of our experiments on LLaMA-7b and LLaMA-2-7b models. The following observations were made: **8-bit Quantization:** The results indicate that 8-bit quantization has a negligible impact on model performance, both for the original and the ASVD-compressed networks. **6-bit Quantization:** A slight degradation in prediction accuracy is observed with 6-bit quantization. This effect is more pronounced in networks with higher compression (lower parameter ratios), suggesting a compounded impact of compression and lower bit quantization. **4-bit Quantization:** Upon quantizing the network into NF4, a further deterioration in prediction accuracy is observed. When param ratio is greater than 0.9, the performance decline attributed to quantization is approximately consistent with that of the non-decomposed network. For instance, in the case of LLaMA-2-7b without decomposition, the NF4 quantization results in a wiki PPL decrease of 0.18 compared to FP16. Similarly, at a param ratio of 0.95, the NF4 quantization yields a PPL decrease of 0.19 compared to FP16. In summary, the findings suggest that ASVD is compatible with weight quantization techniques.

4.5 Decomposed Network Analysis

We conduct a detailed analysis of the decomposed network. Figure 6 presents the per-type parameters ratio and per-block parameters ratio. Observing the plot, we note that parameters in the MLP components (gate projection, up projection, and down projection) exhibit minimal compression. In MHA, the V projection layer experiences relatively small compression, whereas q projection and k projection can be significantly compressed, indicating redundancy in these components. Turning our attention to the per-block compression ratio, we find that the first layer can undergo substantial compression. In contrast, the compression ratios for the other layers, except for two middle layers, show similar compression rates.

5 Conclusion

This study presents a training-free approach to compressing Large Language Models (LLMs). We propose Activation-aware Singular Value Decomposition (ASVD) and Sensitivity-based Truncation Rank Searching (STRS), effectively address the challenges posed by activation outliers and varying layer sensitivities. These techniques enable more accurate and efficient decomposition, reducing memory usage and computational demands while maintaining model performance. The successful integration of ASVD into KV cache compression further underscores its potential for broad applicability and substantial impact in real-world scenarios.

References

- Rishabh Agarwal, Nino Vieillard, Piotr Stanczyk, Sabela Ramos, Matthieu Geist, and Olivier Bachem. Gkd: Generalized knowledge distillation for auto-regressive sequence models. *arXiv preprint arXiv:2306.13649*, 2023.
- Tom Brown, Benjamin Mann, Nick Ryder, Melanie Subbiah, Jared D Kaplan, Prafulla Dhariwal, Arvind Neelakantan, Pranav Shyam, Girish Sastry, Amanda Askell, et al. Language models are few-shot learners. *Advances in neural information processing systems*, 33:1877–1901, 2020.
- Yu Cheng, Duo Wang, Pan Zhou, and Tao Zhang. A survey of model compression and acceleration for deep neural networks. *arXiv preprint arXiv:1710.09282*, 2017.
- Matthieu Courbariaux, Yoshua Bengio, and Jean-Pierre David. Binaryconnect: Training deep neural networks with binary weights during propagations. *Advances in neural information processing systems*, 28, 2015.
- James W Demmel. *Applied numerical linear algebra*. SIAM, 1997.
- Emily L Denton, Wojciech Zaremba, Joan Bruna, Yann LeCun, and Rob Fergus. Exploiting linear structure within convolutional networks for efficient evaluation. *Advances in neural information processing systems*, 27, 2014.
- Tim Dettmers, Mike Lewis, Younes Belkada, and Luke Zettlemoyer. Llm.int8(): 8-bit matrix multiplication for transformers at scale. *arXiv preprint arXiv:2208.07339*, 2022.
- Tim Dettmers, Artidoro Pagnoni, Ari Holtzman, and Luke Zettlemoyer. Qlora: Efficient finetuning of quantized llms. *arXiv preprint arXiv:2305.14314*, 2023.
- Tianyu Ding, Tianyi Chen, Haidong Zhu, Jiachen Jiang, Yiqi Zhong, Jinxin Zhou, Guangzhi Wang, Zhihui Zhu, Ilya Zharkov, and Luming Liang. The efficiency spectrum of large language models: An algorithmic survey. *arXiv preprint arXiv:2312.00678*, 2023.
- Elias Frantar and Dan Alistarh. Sparsegpt: Massive language models can be accurately pruned in one-shot. *ICML*, 2023.
- Elias Frantar, Saleh Ashkboos, Torsten Hoefer, and Dan Alistarh. Gptq: Accurate post-training quantization for generative pre-trained transformers. *arXiv preprint arXiv:2210.17323*, 2022.
- Dan Hendrycks, Collin Burns, Steven Basart, Andy Zou, Mantas Mazeika, Dawn Song, and Jacob Steinhardt. Measuring massive multitask language understanding. *arXiv preprint arXiv:2009.03300*, 2020.
- Geoffrey Hinton, Oriol Vinyals, and Jeff Dean. Distilling the knowledge in a neural network. *arXiv preprint arXiv:1503.02531*, 2015.
- Coleman Hooper, Sehoon Kim, Hiva Mohammadzadeh, Michael W Mahoney, Yakun Sophia Shao, Kurt Keutzer, and Amir Gholami. Kvquant: Towards 10 million context length llm inference with kv cache quantization. *arXiv preprint arXiv:2401.18079*, 2024.
- Yen-Chang Hsu, Ting Hua, Sungen Chang, Qian Lou, Yilin Shen, and Hongxia Jin. Language model compression with weighted low-rank factorization. In *ICLR*, 2022.
- Yani Ioannou, Duncan Robertson, Jamie Shotton, Roberto Cipolla, and Antonio Criminisi. Training cnns with low-rank filters for efficient image classification. *arXiv preprint arXiv:1511.06744*, 2015.
- Max Jaderberg, Andrea Vedaldi, and Andrew Zisserman. Speeding up convolutional neural networks with low rank expansions. *arXiv preprint arXiv:1405.3866*, 2014.
- Mikhail Khodak, Neil Tenenholz, Lester Mackey, and Nicolo Fusi. Initialization and regularization of factorized neural layers. In *ICLR*, 2021.
- Hyeji Kim, Muhammad Umar Karim Khan, and Chong-Min Kyung. Efficient neural network compression. In *Proceedings of the IEEE/CVF conference on computer vision and pattern recognition*, pp. 12569–12577, 2019.

- Sehoon Kim, Coleman Hooper, Amir Gholami, Zhen Dong, Xiuyu Li, Sheng Shen, Michael W Mahoney, and Kurt Keutzer. Squeezellm: Dense-and-sparse quantization. *arXiv preprint arXiv:2306.07629*, 2023.
- Yong-Deok Kim, Eunhyeok Park, Sungjoo Yoo, Taelim Choi, Lu Yang, and Dongjun Shin. Compression of deep convolutional neural networks for fast and low power mobile applications. *arXiv preprint arXiv:1511.06530*, 2015.
- Vadim Lebedev, Yaroslav Ganin, Maksim Rakhuba, Ivan Oseledets, and Victor Lempitsky. Speeding-up convolutional neural networks using fine-tuned cp-decomposition. *arXiv preprint arXiv:1412.6553*, 2014.
- Yann LeCun, John Denker, and Sara Solla. Optimal brain damage. *Advances in neural information processing systems*, 2, 1989.
- Yixiao Li, Yifan Yu, Qingru Zhang, Chen Liang, Pengcheng He, Weizhu Chen, and Tuo Zhao. Lospars: Structured compression of large language models based on low-rank and sparse approximation. 2023.
- Ji Lin, Jiaming Tang, Haotian Tang, Shang Yang, Xingyu Dang, and Song Han. Awq: Activation-aware weight quantization for llm compression and acceleration. *arXiv preprint arXiv:2306.00978*, 2023.
- Zirui Liu, Jiayi Yuan, Hongye Jin, Shaochen Zhong, Zhaozhuo Xu, Vladimir Braverman, Beidi Chen, and Xia Hu Kivi. A tuning-free asymmetric 2bit quantization for kv cache. *arXiv preprint arXiv:2402.02750*, 2024.
- Stephen Merity, Caiming Xiong, James Bradbury, and Richard Socher. Pointer sentinel mixture models. *arXiv preprint arXiv:1609.07843*, 2016.
- Marcin Moczulski, Misha Denil, Jeremy Appleyard, and Nando de Freitas. Acdc: A structured efficient linear layer. *arXiv preprint arXiv:1511.05946*, 2015.
- Ivan V Oseledets. Tensor-train decomposition. *SIAM Journal on Scientific Computing*, 33(5): 2295–2317, 2011.
- Tara N Sainath, Brian Kingsbury, Vikas Sindhwani, Ebru Arisoy, and Bhuvana Ramabhadran. Low-rank matrix factorization for deep neural network training with high-dimensional output targets. In *2013 IEEE international conference on acoustics, speech and signal processing*, pp. 6655–6659. IEEE, 2013.
- Steffen Schotthöfer, Emanuele Zangrando, Jonas Kusch, Gianluca Ceruti, and Francesco Tudisco. Low-rank lottery tickets: finding efficient low-rank neural networks via matrix differential equations. *Advances in Neural Information Processing Systems*, 35:20051–20063, 2022.
- Hugo Touvron, Thibaut Lavril, Gautier Izacard, Xavier Martinet, Marie-Anne Lachaux, Timothée Lacroix, Baptiste Rozière, Naman Goyal, Eric Hambro, Faisal Azhar, et al. Llama: Open and efficient foundation language models. *arXiv preprint arXiv:2302.13971*, 2023a.
- Hugo Touvron, Louis Martin, Kevin Stone, Peter Albert, Amjad Almahairi, Yasmine Babaei, Nikolay Bashlykov, Soumya Batra, Prajjwal Bhargava, Shruti Bhosale, et al. Llama 2: Open foundation and fine-tuned chat models. *arXiv preprint arXiv:2307.09288*, 2023b.
- Ashish Vaswani, Noam Shazeer, Niki Parmar, Jakob Uszkoreit, Llion Jones, Aidan N Gomez, Łukasz Kaiser, and Illia Polosukhin. Attention is all you need. *Advances in neural information processing systems*, 30, 2017.
- Hongyi Wang, Saurabh Agarwal, and Dimitris Papailiopoulos. Pufferfish: Communication-efficient models at no extra cost. *Proceedings of Machine Learning and Systems*, 3:365–386, 2021.
- Xiuying Wei, Yunchen Zhang, Xiangguo Zhang, Ruihao Gong, Shanghang Zhang, Qi Zhang, Fengwei Yu, and Xianglong Liu. Outlier suppression: Pushing the limit of low-bit transformer language models. *Advances in Neural Information Processing Systems*, 2022.

- Wei Wen, Cong Xu, Chunpeng Wu, Yandan Wang, Yiran Chen, and Hai Li. Coordinating filters for faster deep neural networks. In *Proceedings of the IEEE international conference on computer vision*, pp. 658–666, 2017.
- Mingxue Xu, Yao Lei Xu, and Danilo P Mandic. Tensorgpt: Efficient compression of the embedding layer in llms based on the tensor-train decomposition. *arXiv preprint arXiv:2307.00526*, 2023.
- Zhihang Yuan, Lin Niu, Jiawei Liu, Wenyu Liu, Xinggang Wang, Yuzhang Shang, Guangyu Sun, Qiang Wu, Jiaxiang Wu, and Bingzhe Wu. Rptq: Reorder-based post-training quantization for large language models. *arXiv preprint arXiv:2304.01089*, 2023.
- Zhihang Yuan, Yuzhang Shang, Yang Zhou, Zhen Dong, Chenhao Xue, Bingzhe Wu, Zhikai Li, Qingyi Gu, Yong Jae Lee, Yan Yan, et al. Llm inference unveiled: Survey and roofline model insights. *arXiv preprint arXiv:2402.16363*, 2024.
- Xunyu Zhu, Jian Li, Yong Liu, Can Ma, and Weiping Wang. A survey on model compression for large language models. *arXiv preprint arXiv:2308.07633*, 2023.

A Appendix

A.1 Impact Statements and Limitations

In this study, we propose a technique that improves the efficiency of Large Language Models (LLMs), making them more accessible. This approach helps to democratize LLMs by lowering deployment costs and hardware barriers, facilitating their use in edge computing. However, it does not mitigate the potential misuse of LLMs by malicious actors.

A.2 Release Safeguards

While ASVD itself does not release new pretrained models, the compression capabilities it provides could enable easier sharing and deployment of powerful models that have risks of misuse. To mitigate risks of misuse, we have implemented access control. Users must agree to terms prohibiting unethical applications.

A.3 Inference Cost with Decomposed LLMs

Regarding the computational aspect, let's consider the input matrix $\mathbf{X} \in \mathbb{R}^{n \times t}$ and the weight matrix $\mathbf{W} \in \mathbb{R}^{m \times n}$. In the original linear layer, the matrix multiplication is represented as $\mathbf{Y} = \mathbf{X}\mathbf{W}$. The number of Multiply-Accumulate (MAC) operations, denoted as C , in the original linear layer can be computed as: $C = tmn$. After the ASVD decomposition, the matrix multiplication transforms into $\mathbf{Y} = \mathbf{A}_k\mathbf{B}_k$. To analyze the computational efficiency, we calculate the MAC operations, denoted as C_k , for this decomposed form. The computation for C_k is given by: $C_k = tkm + tkn$

This computation ratio can be expressed as the ratio of C_k to C , which is equivalent to the parameter ratio:

$$\frac{C_k}{C} = \frac{km + kn}{nm} \quad (6)$$

Remarkably, this computation ratio mirrors the weight number compression ratio, highlighting the efficient use of computational resources achieved through ASVD. In summary, ASVD can not only reduce the weight storage and weight transferring overheads in LLM deployment but also reduce the computation required by LLM inference.

A.4 Binary Search for Truncation Ranks

We have the option to employ either a performance target or parameters target for our search. In the case of a performance target, our objective is to identify the truncation rank configuration that ensures the compressed network attains the desired performance, such as achieving a specific perplexity. Alternatively, in the pursuit of a parameters target, our goal is to identify the truncation ranks that result in the network attaining the specified target parameters.

The algorithm of performance target: Initially, the low pointer (p_L) is positioned at the start of the list, while the high pointer (p_H) is set at the list's end. The middle pointer (p_M), as the name suggests, is placed midway between p_L and p_H , calculated as $p_M = \lfloor \frac{p_L + p_H}{2} \rfloor$. During each iteration of the binary search, we adjust the truncation rank for each layer. Specifically, for a given layer, its truncation rank is set to the smallest rank found to the right of the middle pointer (p_M) in our list.

Following this adjustment, we evaluate the network's performance using the updated configuration on a calibration dataset. The primary metric for assessment is perplexity. Should the perplexity fall within or below a pre-established threshold, we move the high pointer (p_H) to the middle position (p_M). This action indicates our search for a configuration with a potentially lower rank that still adheres to performance standards. Conversely, if the perplexity exceeds our maximum acceptable threshold, we shift the low pointer (p_L) to ($p_M + 1$). This adjustment signifies the need to increase the truncation ranks to maintain or enhance performance levels. The binary searching will converge to an optimal configuration of truncation ranks for each layer that balances compression ratio and perplexity.

The algorithm of parameters target is shown in Algorithm 1. It doesn't need calibration dataset.

Algorithm 1: Binary Search for Truncation Ranks (parameters target)

Input: List of tuples (layer, truncation rank, sensitivity) and parameters target

Output: Optimal truncation rank configuration for each layer

Sort the list by sensitivity in ascending order

Initialize pointers: $p_L = 0$, $p_H = \text{length of list} - 1$

```
 $p_M = \lfloor \frac{p_L + p_H}{2} \rfloor$ 
while  $p_L \neq p_H$  do
  for each layer in the list do
    Initialize  $r = \infty$ 
    for each tuple in the list starting from  $p_M$  to the end do
      if tuple's layer is the same as the current layer then
         $r = \min(r, \text{tuple's truncation rank})$ 
      end if
    end for
    if  $r = \infty$  then
      Do not modify the truncation rank for the layer
    else
      Set the truncation rank for the layer to  $r$ 
    end if
  end for
  Calculate the parameters after compression
  if parameters  $\leq$  parameters target then
     $p_H = p_M$ 
  else
     $p_L = p_M + 1$ 
  end if
  Update  $p_M = \lfloor \frac{p_L + p_H}{2} \rfloor$ 
end while
```

A.5 Difference with TensorGPT [Xu et al. \[2023\]](#).

In the content of LLM compression via decomposition, the most related work is the concurrent TensorGPT [Xu et al. \[2023\]](#), [Zhu et al. \[2023\]](#), in which the embedding layer of LLMs is compressed through Tensor-Train Decomposition (TTD) [Oseledets \[2011\]](#) in order to store large embeddings in a low-rank tensor format, with much fewer parameters. However, there are several differences between those two methods: (1) Unlike TensorGPT which focuses solely on the token embedding matrix, ASVD aims to compress the entire weight spectrum of LLMs. This holistic approach addresses a more critical aspect of LLM compression, as highlighted in recent studies [Kim et al. \[2023\]](#), [Lin et al. \[2023\]](#); (2) From the perspective of low-rank decomposition categorization, our method can realize the low-rank decomposition in a rank-adaptive manner, contrasting with the fixed or predetermined ranks used in TensorGPT.

A.6 Empirical Comparison with FWSVD

We also compare ASVD with FWSVD [Hsu et al. \[2022\]](#), which uses Fisher information to weigh the importance of parameters affecting the model prediction. Note that FWSVD is training-required. As shown in Table 4, our method can outperform FWSVD comprehensively.

A.7 Hyper-parameters Exploration

In our study, we initiate an exploration of hyper-parameters in ASVD, focusing on the activation channel significance metric and the control factor α . This exploration is conducted on OPT-125m, a relatively small network that facilitates rapid evaluation.

We rigorously explored the control factor α at various settings: 0.1, 0.25, 0.5, 1, and 2. This exploration aimed to understand how varying α influences the performance and parameter efficiency of the network. Additionally, we investigated two methods for quantifying activation significance: Absolute Mean Value of Input Activation and Absolute Maximum Value of Input Activation. These

Table 4: Comparing with FWSVD on LLaMA-7b. FWSVD* denotes Fisher information weighted SVD.

param ratio		0.95	0.9	0.85	0.8
LLaMA-7b					
FWSVD+STRS	wiki	5.86	6.32	7.48	10.70
ASVD		5.78	6.09	6.80	8.89
FWSVD+STRS	ptb	34.33	38.05	58.75	125.80
ASVD		32.64	37.80	52.11	88.09
LLaMA-2-7b					
FWSVD+STRS	wiki	5.59	6.12	8.01	13.07
ASVD		5.64	5.93	6.74	8.91
FWSVD+STRS	ptb	25.06	36.58	105.53	222.03
ASVD		23.98	32.63	59.84	114.70

Table 5: Perplexity on Wikitext2 for exploring hyper-parameters on OPT-125m.

α	0.1	0.25	0.5	1	2
SVD+STRS			103.39		
ASVD abs mean	47.54	37.12	36.89	41.53	43.81
ASVD abs max	52.63	47.17	40.14	41.94	52.55

methods are crucial in determining the most effective approach for activation channel significance evaluation. We set a target parameters ratio of 0.9. Utilizing the binary search approach for truncation ranks, we report the perplexity on Wikitext2 test set after compression. The results of our experiments are summarized in Table 5.

From the data presented in the table, we observe that both activation-aware methods show superior performance compared to standard SVD+STRS. We also notice that Lower and higher values of α (0.1 and 2) exhibit lower performance, while mid-range values (0.5) lead to better performance, and the Absolute Mean Value method consistently outperforms the Absolute Max Value method. Therefore, based on our observations, we chose $\alpha = 0.5$ and the Absolute Mean Value method for setting the scaling matrix S in the ASVD process in the following experiments.

A.8 Absorbing Singular Values

Table 6: Perplexity on Wikitext-2 under different absorbing strategies after ASVD on OPT-125m.

param ratio	weight quant	absorbed by U	absorbed by V	absorbed by V
0.9	INT6	37.58	39.67	40.62
0.85	INT6	60.44	64.19	61.02

After we decompose a matrix via ASVD, we can represent the weight matrix as a product of three matrices, i.e., $\mathbf{W} \approx \mathbf{U}_k \mathbf{\Sigma}_k \mathbf{V}_k^T$. Thanks to the diagonal nature of matrix $\mathbf{\Sigma}_k$, we can further optimize the inference process. Specifically, we can efficiently absorb the singular values in $\mathbf{\Sigma}_k$ into the matrices \mathbf{U}_k and \mathbf{V}_k^T . We achieve this fusion using the following strategy: $\mathbf{A}_k = \mathbf{U}_k \sqrt{\mathbf{\Sigma}_k}$ and $\mathbf{B}_k = \sqrt{\mathbf{\Sigma}_k} \mathbf{V}_k^T$. Consequently, we obtain a more computationally efficient matrix operation²:

$$\mathbf{Y} = \mathbf{W}\mathbf{X} \approx \mathbf{A}_k(\mathbf{B}_k\mathbf{X}) \quad (7)$$

Compared to the methods of fusing the singular values $\mathbf{\Sigma}_k$ solely into either \mathbf{U} or \mathbf{V} matrices, our proposed fusion technique offers significant advantages in terms of weight quantization, as demonstrated in Table 6. Our approach involves evenly distributing the singular values from the diagonal matrix $\mathbf{\Sigma}_k$ into both \mathbf{U}_k and \mathbf{V}_k^T matrices. This ensures a more uniform distribution of \mathbf{A}_k and \mathbf{B}_k , leading to a reduction in the disparity across different channels and reducing the quantization error.

²See Appendix for details.